Using CFD to Predict Inspired CO_2 and O_2 after Ventilation Shutoff During a Gateway Emergency Response or Maintenance

Marshall C. McCray[1] and Rachel A. Sturtz[2]
Jacobs JETS, Houston, Texas, 77058

On Gateway there are several emergency or maintenance scenarios where ventilation will be completely or partially shut off. In response to a cabin fire or toxic atmosphere, cabin intramodular ventilation and intermodule ventilation (IMV) is ceased to limit the spread of toxins. Ventilation is temporarily shut off during emergency depressurization to aid in using the hatch air direction indicator to locate the source of the leak. There are also several routine and off-nominal maintenance tasks that require complete or partial ventilation shutoff. To ensure a safe environment for the crew while ventilation is off, a computational fluid dynamics (CFD) model was developed to evaluate local concentration buildup of CO_2 and depletion of O_2 that arise from crewmember respiration. The model simulated a spherical crewmember's head with realistic breathing patterns and tracked how inhaled concentrations changed over time after the fans were shut off. A variety of turbulence models, mesh sizes, crew location, and number of crew within the module were assessed. The model was used to predict the time-to-effect for crewmembers to inhale dangerous levels of CO_2 or O_2. Results showed the partial pressure of CO_2 inspired for a single crewmember in habitation and lunar outpost (HALO) reached 10 mmHg after 2 hours, and for two crew the same concentration was reached in 1.4 hours.

Acronyms and Nomenclature

A_m	=	mouth area
CFD	=	computational fluid dynamics
CO_2	=	carbon dioxide
ϵ	=	rate of dissipation of turbulent kinetic energy
HALO	=	Habitation and Lunar Outpost
HARS	=	HALO Air Revitalization System
H_2O	=	water vapor
IMV	=	intermodular ventilation
k	=	turbulent kinetic energy
m_{ex}	=	total mass of exhaled gases per breath period
$\dot{m}$	=	mass flow rate
N_2	=	diatomic nitrogen
O_2	=	diatomic oxygen
pp	=	partial pressure
RANS	=	Reynolds-Averaged Navier-Stokes
ρ_m	=	density computed at mouth surface
SST	=	shear stress transport
t	=	time
T_b	=	breath period
ω	=	specific rate of dissipation of turbulent kinetic energy to thermal energy

[1] Thermal Analysis Engineer, Thermal, Fluids and Life Support Analysis JE33, 5E04 2224 Bay Area Blvd. Houston, TX, 77058.
[2] Modeling and Simulation Chemical Engineer, Thermal, Fluids and Life Support Analysis JE33, 5E04 2224 Bay Area Blvd. Houston, TX, 77058.

v_m	=	mouth velocity
V_T	=	tidal volume

I. Introduction

VENTILATION in a crewed space environment is vital to ensure the health and safety of the crew. A ventilation system delivers fresh, oxygenated air to the crew and provides flow to wash away high carbon dioxide (CO_2) concentrations exhaled by the crew. During nominal operations, there are two main forms of ventilation provided: intramodule and intermodule. Intramodule ventilation is provided by cabin fans, which circulate air within the module to ensure a well-mixed cabin volume and return the air to the module's Air Revitalization System (ARS) for conditioning. Intermodule ventilation (IMV) is supplied by IMV fans, which provide mixing between adjacent modules. IMV fans force air from module A to module B resulting in airflow through the open hatch from module B to module A.

There are some contingency and off-nominal scenarios where partial or full ventilation shutdown is necessary. In a contingency event such as a fire or chemical spill, both IMV and intramodule ventilation will be turned off to limit the spread of smoke and toxins. In the event a cabin leak is detected, ventilation may need to be temporarily turned off to facilitate locating the leak.

This analysis focuses on evaluating crew safety in Gateway's Habitation and Logistics Outpost (HALO) module after both intramodule ventilation and IMV are turned off. Intramodule ventilation on HALO is provided by cabin fans in the HALO Air Revitalization System (HARS). HARS controls temperature, humidity, and oxygen (O_2) levels for HALO. HALO nominally relies on IMV to the Lunar I-Hab module for CO_2 removal. Without ventilation, the crew does not receive conditioned air and pockets of low O_2 and high CO_2 may form around the crewmember's face.

A computational fluid dynamics (CFD) model of HALO's habitable volume was used to analyze O_2 and CO_2 concentrations inhaled by crewmembers after ventilation was shut off. The model simulates a crewmember with a realistic metabolic profile and breathing pattern at multiple locations within the HALO cabin. The results are used to determine how long crew can be in a module without ventilation before there are risks of hypoxia and/or hypercapnia. The results from the study will be used to inform flight rules and help determine the necessity of additional emergency equipment.

II. Background

Previous assessments of CO_2 buildup and O_2 depletion after fans shut off modeled the crewmember as a small sphere. The results using this method suggested that CO_2 limits were reached within 40 seconds, however this was determined overly conservative and unrealistic in the way it inhaled and exhaled in all directions. The efforts of this analysis were focused on modeling the crew more realistically.

Human-generated CO_2 buildup has also been analyzed with CFD for ventilated International Space Station modules.[1] In this model, CO_2 was generated from a point-source at a constant rate using a 10 second timestep. Isosurfaces of CO_2 concentrations in the module were plotted to understand locations where high levels CO_2 developed. Although this analysis demonstrated that regions of high CO_2 concentrations could develop over time in a microgravity environment, it did not account for a ventilation-off scenario or a realistic inhale/exhale breathing pattern through a directional mouth or nostrils.

III. Methodology

A Reynolds-Averaged Navier-Stokes (RANS) CFD model was developed in Ansys Fluent to simulate the evolution of CO_2 and O_2 concentrations over time in the HALO cabin after ventilation is turned off. The crewmember breathes throughout the simulation, consuming O_2 and producing CO_2 and water vapor. The ventilation is on for a short period before turning off at ~23 s. After ventilation stops, the vents in the CFD domain are removed to reduce cell count. This section summarizes the major modeling choices for geometry, mesh, physics, and solver settings.

A. HALO Cabin Model

This analysis used a simplified internal geometry of HALO, which consists of the habitable volume of HALO and the supply/return vents which connect to HALO's ventilation system and HARS. There are six vents that supply airflow to the HALO cabin and seven vents that return air back to the HARS and one vent that connects the axial IMV to the Lunar I-HAB. There are three hatchways where the axial hatchway flows into HALO and the two radial hatchways flow out of HALO. The two radial IMVs are ducted directly into HALO's ventilation system. Figure 1 shows the simplification of the ventilation system to only include the vents in the CFD domain. Space behind equipment closeout panels was not included in the domain.

HALO will be docked to the Gateway stack with hatchways open during nominal operations. To simplify

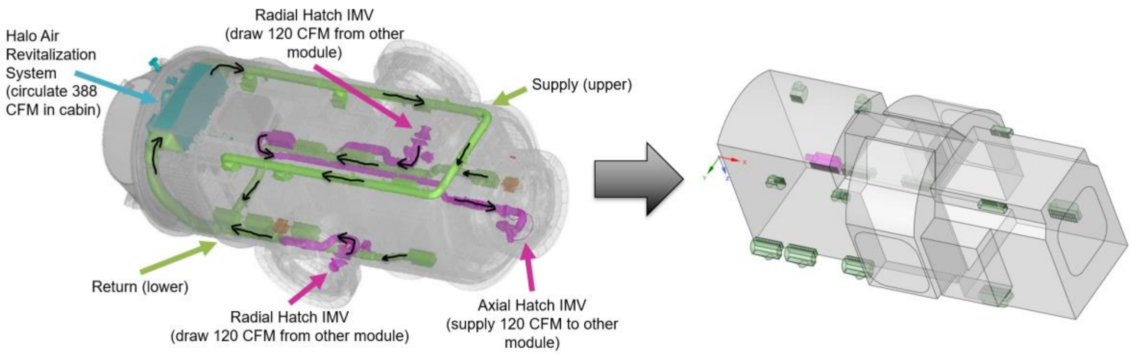

a) HALO module with ventilation loop b) Simplified domain for CFD

Figure 1. Simplification of HALO ventilation loop (a) for CFD domain with vents (b).

computations, the hatchways were modeled using velocity boundaries instead of including neighboring modules in the computational domain. Velocity boundary conditions were assigned to the vents and hatchways labeled in Figure 2 on the volumetric flow rates listed in Table 1.

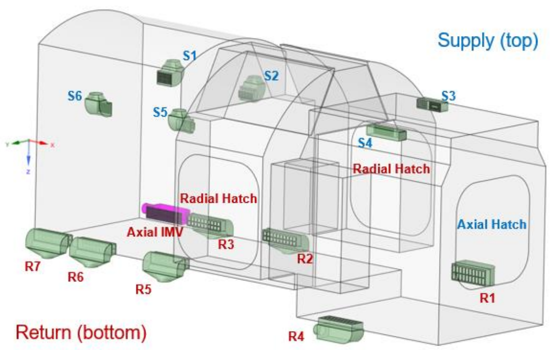

Figure 2. Flow boundaries for computational domain.

Table 1. Flow rates for HALO ventilation registers.

Label	Vdot [CFM]	Vdot [m³/s]	Area [m²]	Vel [m/s]	BC Type
S3	68	0.0321	0.0258	1.2425	inlet
S4	55	0.0260	0.0354	0.7339	inlet
S2	98	0.0463	0.0126	3.6806	inlet
S5	41	0.0193	0.0126	1.5398	inlet
S1	66	0.0311	0.0126	2.4788	inlet
S6	60	0.0283	0.0126	2.2535	inlet
R3	26	0.0123	0.0437	0.2809	outlet
R2	19	0.0090	0.0437	0.2053	outlet
R1	18	0.0085	0.0655	0.1296	outlet
R7	30	0.0142	0.0437	0.3241	outlet
R6	26	0.0123	0.0437	0.2809	outlet
R5	22	0.0104	0.0437	0.2377	outlet
R4	21	0.0099	0.0655	0.1512	outlet
Axial IMV	120	0.0566	0.0494	1.1469	outlet
Radial Hatch	120	0.0566	0.9943	0.0570	outlet
Axial Hatch	~120	~0.0566	~0.9867	~0.0574	pressure inlet

Velocity boundary conditions are enforced at the ducting cutoff and are based on the register's flow rate and ducting area, depicted in Figure 3.

The radial hatchways were modeled as velocity boundaries with flow rates equal and opposite to the IMV flow

Figure 3. Location of velocity boundary condition on ventilation register.

rates. The axial hatchway was modeled using a pressure inlet, allowing its flow rate to fluctuate as needed to maintain cabin pressure. This ensured that the cabin did not pressurize or depressurize during the ventilation-on period. Figure 4 demonstrates the effect the IMV flow has on the hatchways.

Ventilation was on for the first 23.28 s of the simulation. This allowed six full breath periods to occur, allowing the domain to reach a steady air flow field. Starting at 23.28 s the flow at the boundaries decreased linearly for one second, until the velocities reached zero at 24.28 s. Figure 5 shows the cabin-average velocity magnitude decay after ventilation shutoff.

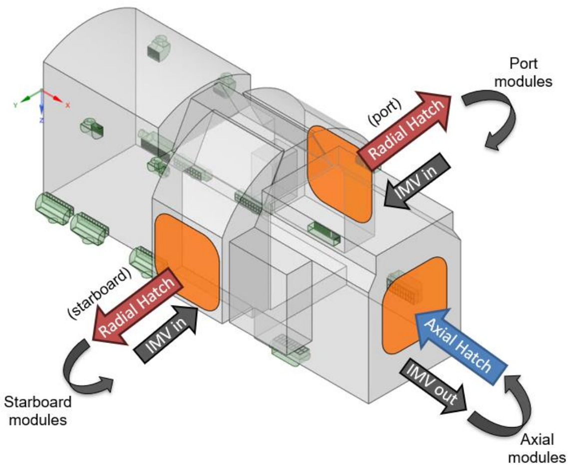

Figure 4. Flow through HALO hatchways caused by IMV circulation.

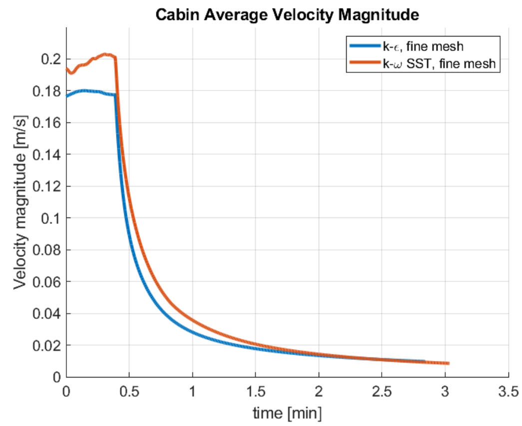

Figure 5. Decay of air flow velocity after ventilation shutoff.

The cabin was initialized with "fresh" air, based on Gateway Integrated ECLSS Model simulation results for nominal awake conditions (well-mixed). These same partial pressures were used to define the quality of the air coming out of the vents in the CFD boundary conditions. Table 2 lists the partial pressure of each species for initialization and inlet boundary conditions.

Table 2. Partial pressures of constituents for ventilation boundary conditions and initial cabin environment.

ppO_2	$ppCO_2$	ppH_2O	ppN_2
147 mmHg	2.00 mmHg	5.26 mmHg	373 mmHg
(19600 Pa)	(267 Pa)	(701 Pa)	(49700 Pa)

Although most of the domain was simplified, the detail on the vent geometry was maintained, as it influenced how air flows into the domain. These vent registers are included in the CFD domain during the ventilation-on period (first 23.28 s). Vents account for 75 percent of the mesh cell count despite representing only 0.6 percent of the domain volume. The vents were found to be a significant contributor to slowing down the simulation, and their influence on the cabin domain after fans are off is negligible. To reduce computational effort without compromising accuracy, the vents are removed from the domain after ventilation turns off. This is done by imposing the solution from the domain with vents onto the simplified domain and then continuing the simulation. This simplification was found to produce a 3.9x speedup in simulation time. Figure 6 depicts the simplified domain with a small (0.1 m × 0.1 m × 0.1 m) pressure outlet added for numerical stability. A new pressure outlet was added because the other boundaries were switched to walls, including the axial hatchway which originally served as the pressure outlet. This allows gas to exit the

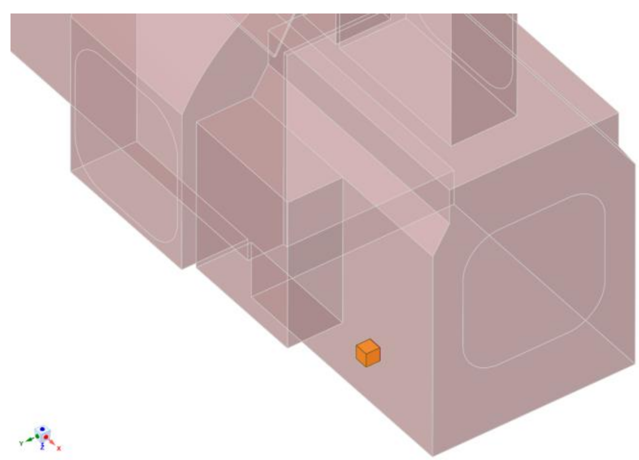

Figure 6. Simplified fluid domain with pressure outlet.

domain during exhales and enter the domain during inhales. For reversed flow on the pressure outlet during inhales, the species mass fractions (concentrations) were set equal to the mass fractions from the last timestep of the exhale period. This simple boundary condition does not guarantee perfect mass conservation of each species returning to the domain but returns air with similar concentrations to what left the domain during the exhale.

B. Crewmember Representation

Breathing crewmembers were modeled as stationary, spherical heads with flat, circular mouths of area 0.0004918 m^2. Figure 7 depicts the geometric representation of a crewmember in the CFD domain. Previous CFD efforts modelled crew as small, spherical orbs with the same surface area as the flat circular mouth. However, that geometry resulted in unrealistically high levels of CO_2 inspired because the breath plume lingered close to the orb due to a lack of uni-directional momentum.

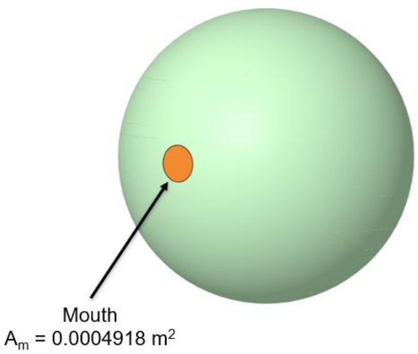

Figure 7. Model of crewmember head and mouth.

Table 3. Metabolic profile of breathing crewmember.

Gender	Male
Aerobic fitness statistic	95%
Metabolic rate	549.5 BTU/hr (161.0 W)
Tidal volume	1.027 L/breath
Respiratory rate	15.49 breaths/min

C. Metabolic Profile and Breathing Pattern

Test data[2] correlates metabolic rate, tidal volume, and respiratory rate to subjects' aerobic fitness level, gender, and metabolic rate. The profile of a 95th percentile, high fitness level male at nominal awake conditions is listed in Table 3.

The time-averaged physiological crewmember profile information (metabolic rate, respiratory rate, and tidal volume) is used to create a semi-realistic, sinusoidal breathing pattern[3] in time with O_2 consumption and CO_2 and H_2O production that matches the profile. The respiratory rate, tidal volume, and metabolic rate are assumed to be constant throughout the simulation. Also, the inhale and exhale periods are assumed to take equal time, each half of the breath period.

The tidal volume is defined as the lung capacity and therefore must be equal to the integral of the volumetric flow rate over the inhale period, as expressed in Eq. (1).

$$V_T = \int_0^{T_b/2} A_m v_m(t)dt \tag{1}$$

The volumetric flowrate at the mouth during the inhale period is assumed sinusoidal with period T_b. Solving for the amplitude which satisfies Eq. (1) results in the mouth velocity during each inhale period,

$$v_m(t) = \frac{V_T \pi}{A_m T_b} sin\left(\frac{2\pi}{T_b} t\right). \tag{2}$$

The mass flow rate of each species is integrated over each timestep of the inhale period, resulting in a final inhaled mass of each species. After the inhale period is completed, but before exhale occurs, lung contents are updated based on the crewmember's metabolic profile. New "exhale" masses are computed for each gas constituent in the lungs. O_2 is removed and CO_2 is added to the domain based on the metabolic profile of the crewmember. The gas inside the lungs is assumed to heat up to the crewmember's body temperature of 98.3°F (310 K). H_2O is added such that relative humidity of the exhale is 100 percent. Nitrogen is conserved.

The mouth velocity during the exhale ensures that the mass of the gas in the lungs is completely exhaled, as enforced by Eq. (3).

$$m_{ex} = \int_{T_b/2}^{T_b} \dot{m}(t)dt \tag{3}$$

The mass flow rate at the mouth during the exhale period is assumed sinusoidal with period T_b. Exhaled constituents are assumed to be well-mixed in the lungs, leading to constant concentrations of each constituent over a given exhale period. Solving for the amplitude which satisfies Eq. (3) results in the mass flow rate during each exhale period.

$$\dot{m}(t) = -\frac{m_{ex}\pi}{T_b} sin\left(\frac{2\pi}{T_b}t\right) \tag{4}$$

The mouth velocity for exhaling is then calculated from dividing the mass flow rate $\dot{m}(t)$ by the density at the mouth surface $\rho(t)$ and area of the mouth A_m,

$$v_m(t) = \frac{m_{ex}\pi}{T_b A_m \rho_m(t)} sin\left(\frac{2\pi}{T_b}t\right). \tag{5}$$

Only the mouth velocity and mass fractions for each species are passed to Fluent at each timestep. In reality, the concentration of CO_2 would increase toward the end of an exhale due to the "dead space" in the respiratory system that does not participate in gas exchange.[4] In this simplified model, however, exhaled concentrations are assumed constant during an exhale period. These mass fractions are calculated from the masses of each constituent divided by m_{ex} and are passed to Fluent as boundary conditions. The inhale velocity has the same amplitude for each inhale period since it is based on a constant tidal volume. However, the exhale velocity amplitude depends on the lung contents and density on the mouth boundary, which varies from breath to breath. Figure 8 shows the variation of mouth velocity vs time.

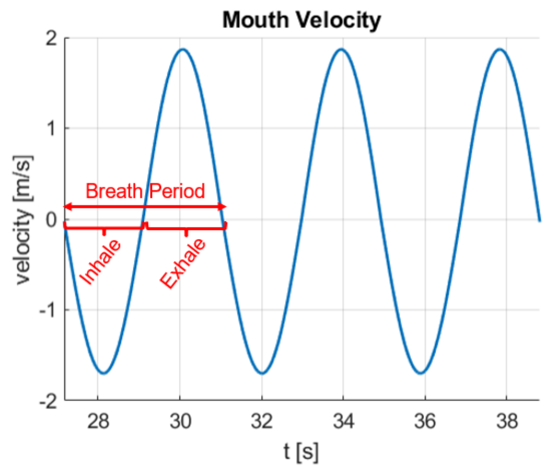

Figure 8. Mouth velocity variation with time.

Exhale flow reached a Reynolds number of 1700, indicative of laminar flow. However, studies show that turbulence may develop in the trachea.[5] Therefore, exhales were assumed to be turbulent, but with relatively low turbulence. Since the exhaled breath is similar to an axisymmetric jet, a turbulent intensity of 2 percent and turbulent length scale of 7.5 percent of the mouth radius was assigned.[6] Figure 9 depicts the velocity magnitude of the breath plume near peak exhale with in-plane vectors to visualize flow direction.

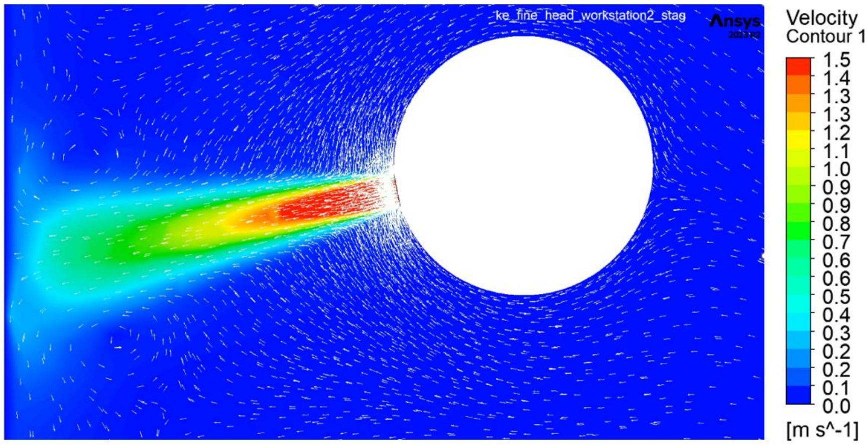

Figure 9. Velocity contour of breath plume, peak exhale.

D. Mesh

Tetrahedral meshes for the CFD simulations were generated using local cell sizing. This ensured that the details near vents had sufficient resolution while the larger cabin volume contained larger cells to improve computational efficiency. Figure 10 shows the detail of the surface mesh of a vent supply register. These portions of the mesh were removed from the domain once the ventilation was turned off.

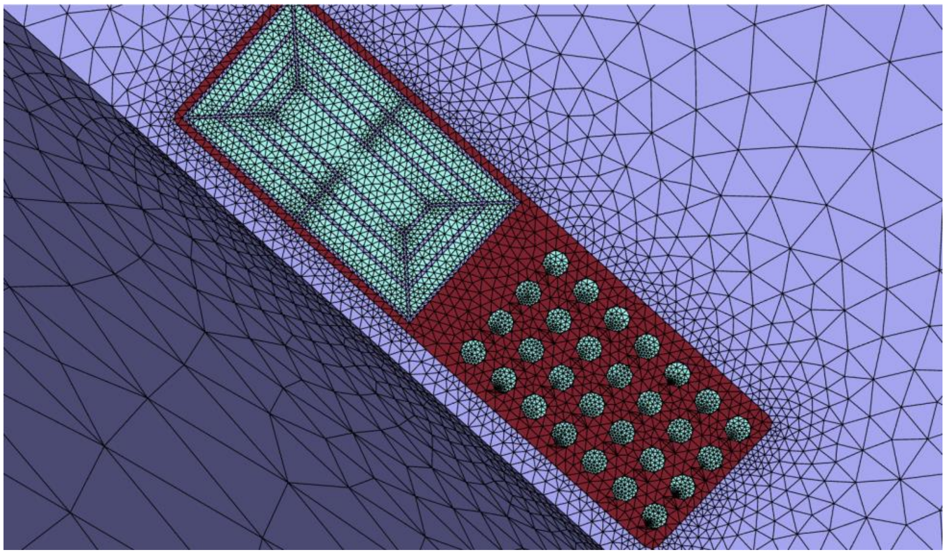

Figure 10. Surface mesh of HALO vent supply register.

Cell sizing was reduced around the head and mouth to capture flow details near the crewmember. Figure 11 shows the cross-section of a tetrahedral mesh with the crewmember highlighted. Tetrahedral meshes were later converted to polyhedral meshes to reduce cell count and computation time.

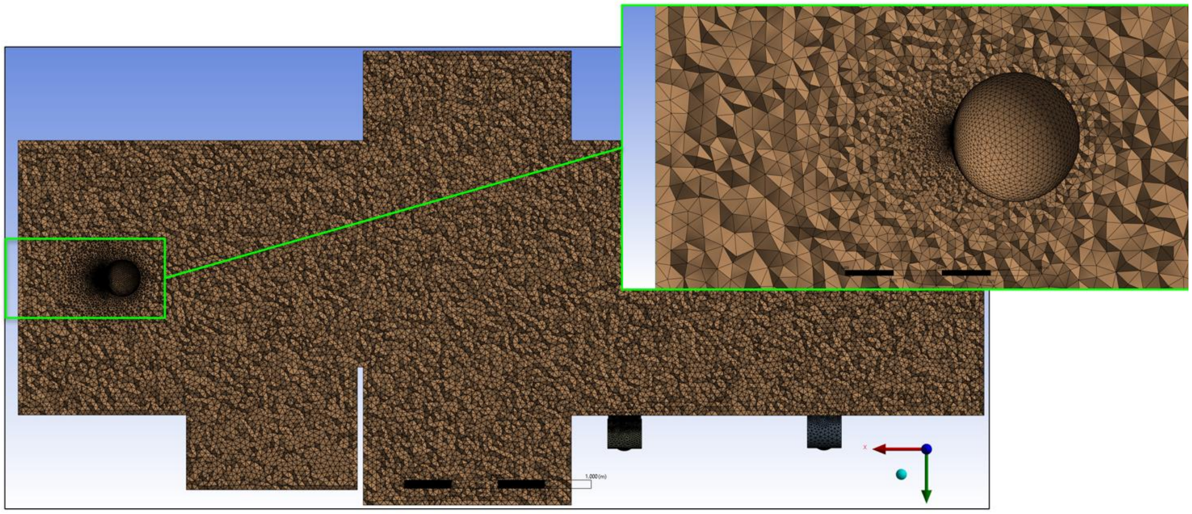

Figure 11. Cross-sectional view of a tetrahedral mesh.

A mesh independence study was conducted to determine solution sensitivity to mesh resolution. Increasing cell count should theoretically improve solution accuracy. Figure 12 shows that the partial pressure of CO_2 inspired converges on a solution as cell count increases. However, higher cell count significantly slows down the simulation. Based on this study, a mesh with cell count of 2.3 million polyhedral cells was chosen for the analysis.

E. Turbulence Model

The $k - \epsilon$ and $k - \omega$ SST turbulence models were chosen to model turbulence in the CFD simulation due to their proven accuracy and widespread use. Without human-in-the-loop testing it would be difficult to determine which model is more accurate. Therefore, both turbulence models were analyzed.

F. Solver Settings

An incompressible, pressure-based solver with 2nd order spatial and temporal discretization was used in Fluent. Time steps ranging from 0.01 s to 0.05 s were found to produce similar results and required roughly the same amount of computational effort. Most results included in this report used a timestep of 0.01 s.

Convergence criteria for each timestep was enforced for each flow variable. Density, pressure, velocity components (x, y, z), and turbulent kinetic energy, ϵ (or ω) were set to Fluent's default convergence criteria of 1e-3. Energy and species were set to 1e-6. The turbulent dissipation variables (ϵ for $k - \epsilon$ model and ω for $k - \omega$ SST model) were typically the last variables to converge. Stricter convergence criteria of 1e-4 were tested with significant computational impact but minimal improvement in accuracy, so they were not used.

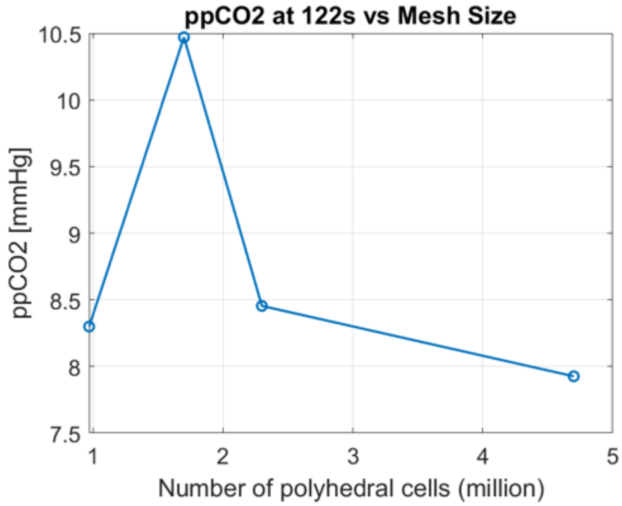

Figure 12. Mesh sensitivity study using partial pressure of CO_2 inhaled as solution parameter.

IV. Results

The time-to-effect for dangerous CO_2 and O_2 levels inspired by crewmembers at various locations inside the HALO module are discussed in this section. Results from both the $k - \epsilon$ and $k - \omega$ SST turbulence models are analyzed. Some other changes such as time step, convergence criteria, and a two-person case are also discussed.

The Gateway Subsystem Specification for the Environmental Control and Life Support Subsystem (ECLSS), GP-10004[7] was referenced for CO_2 and O_2 limits. L2-ECLS-0811 CO_2 Partial Pressure Control – Off-nominal, provides maximum allowable exposure times to various CO_2 concentration ranges, as listed in Table 4. While exposure to high concentrations of CO_2 is a concern, the possibility of hypoxia, or lack of oxygen, is of equal concern. L2-ECLS-0119 Minimum Oxygen Content defines 127 mmHg as the minimum allowable partial pressure of O_2 inspired by crewmembers.

Table 4. GP-10004 maximum allowable inspired $ppCO_2$ levels.

$ppCO_2$ (kPa)	$ppCO_2$ (mmHg)	Exposure Time
0 - Nominal	0 - Nominal	Indefinite
Nominal - 0.9	Nominal - 6.8	8 hours
0.9 - 1.3	6.8 - 10	4 hours
1.3 - 2.0	10 - 15	1 hour

G. Crewmember breathing locations

A variety of crewmember locations were chosen to assess the impact of location on inhaled ppO_2 and $ppCO_2$. In reality, crewmembers could move about the module during an emergency. Body translation would mix the air and head rotation would reduce the likelihood of concentrated CO_2 pockets forming near the face. However, each breathing head in this CFD model remained stationary during the simulation. This choice was made for conservatism on inhaled ppO_2 and $ppCO_2$ to reduce additional variables (such as movement path, rotation angles, and velocities), and avoid the complexities of implementing moving meshes in the simulation.

To understand how inspired concentrations vary with location and proximity to walls, eight different orientations were tested separately. The various locations are depicted in Figure 13.

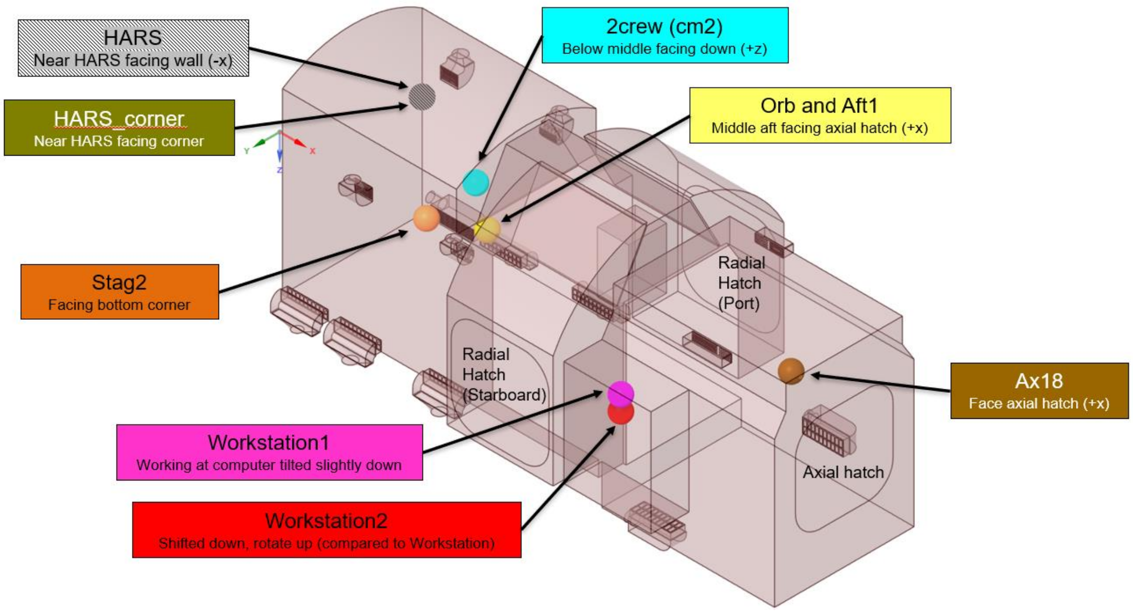

Figure 13. Crew breathing locations.

Breathing locations were selected to represent possible scenarios during an emergency or maintenance tasks. For instance, the locations labeled "workstation1" and "workstation2" were chosen to represent a crewmember monitoring information on the laptop located in that area. These two heads vary slightly in height and are angled slightly differently to capture sensitivity of CO_2 inspired to orientation adjustments. The "HARS" and "HARS_corner" crewmembers are positioned arms-length from the wall near the HARS unit. The "HARS" crewmember faces directly at the wall while "HARS_corner" faces the corner of the module. The "Aft1" crew location represents a crewmember breathing in the center of the module, away from walls. "Stag2" represents a crewmember breathing directly into the lower corner of the module where three walls meet. In this particular case, the domain was initialized with zero air flow (no ventilation) and assessed this breathing location with the expectation that a pocket of high CO_2 concentration would form, and perhaps serve as a worst-case scenario for time-to-effect of CO_2 buildup. "Ax18" represents a crewmember positioned 18 in (0.46 m) away from and facing the axial hatch.

One simulation included two crewmembers breathing at the same time to assess the impact of another crewmember within the vicinity. This scenario used one crewmember in the "HARS" orientation and the other in the "2crew" orientation. Results from this case can be directly compared to the equivalent case with one crewmember ("HARS" only) to understand how increasing the number of crew would impact the gas concentrations inhaled over time.

H. Short-term results (t < 10 min)

Within the first 10 minutes after ventilation stops, both breathing location and turbulence model were found to highly impact inhaled $ppCO_2$ and ppO_2. Figure 14 shows the flowrate-weighted average partial pressure of CO_2 inspired over time for various breathing locations. The volume-averaged $ppCO_2$ in the entire cabin is plotted in dashes, which highlights that inspired levels are much higher than the volume-averaged $ppCO_2$. Each case represents a separate simulation of a single crewmember breathing in the domain. Even a slight shift in breathing orientation can impact results.

Figure 15 demonstrates how a slight change in breathing orientation affects the local O_2 concentrations in the region.

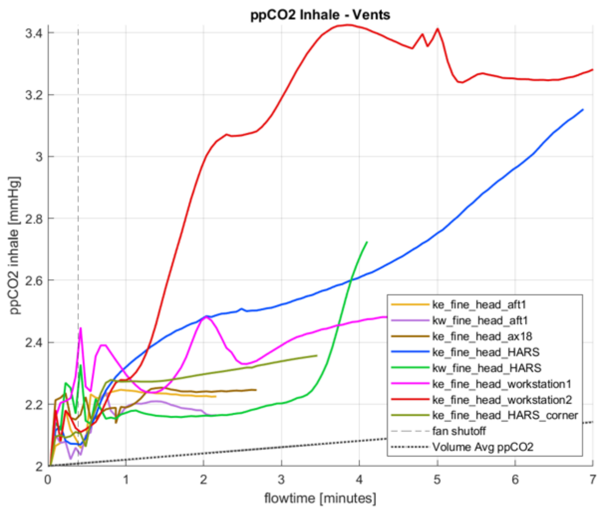

Figure 14. Partial pressure of CO_2 inspired short-term results.

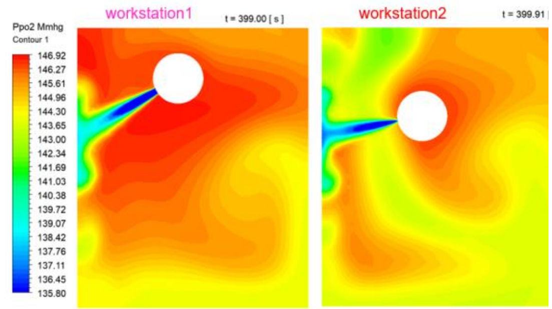

a) ppO_2 workstation 1 b) ppO_2 workstation 2

Figure 15. Partial pressure of O_2 in HALO workstation area for two different breathing.

Within this timeframe, the maximum concentration of $ppCO_2$ inspired for these eight cases was 3.4 mmHg. While 3.4 mmHg (453 Pa) $ppCO_2$ exceeds nominal levels, it does not exceed the maximum allowable exposure time for this concentration as outlined in Table 4. The lowest O_2 level for these short-term results was 144.5 mmHg (19265 Pa)- well above the minimum limit. While no $ppCO_2$ or ppO_2 limits were exceeded within this timeframe, no trends between location or turbulence model could be identified. Additionally, no generalization of time-to-effect could be extrapolated from these short-term results due to their unpredictability. Longer cases were needed to evaluate time-to-effect.

I. Effective Mass Diffusion

Mass diffusion is the movement of particles due to gradients in concentrations. When ventilation ceases in HALO, gases spread in the cabin as a function of effective diffusion, which is characterized by both molecular and turbulent diffusion. Molecular diffusion occurs due to the random motion of particles, whereas turbulent diffusion arises directly from turbulent kinetic energy k and has a much greater impact on the effective diffusion. It follows that the turbulence model, which is responsible for calculating k, directly influences how the CO_2 diffuses in the cabin.

The $k - \epsilon$ model typically generated more turbulent kinetic energy, resulting in higher effective diffusion of exhaled gases near the crewmembers, whereas he $k - \omega$ SST model was found to generate less turbulent kinetic energy, resulting in lower diffusion and therefore higher local concentrations of CO_2 near the crewmembers.

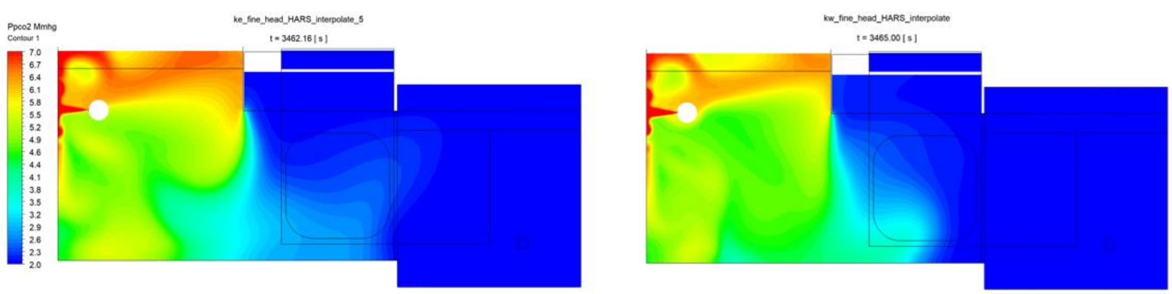

a) $ppCO_2$ with $\boldsymbol{k - \epsilon}$ turbulence model b) $ppCO_2$ with $\boldsymbol{k - \omega}$ SST turbulence model

Figure 16. $ppCO_2$ contours, 1 hour after fan shutoff.

Figure 16 depicts a contour of the partial pressure of CO_2 in the cabin after 1 hour. Despite the slight differences in concentrations, the CO_2 exhaled by the crewmember did not travel the length of the cabin after 1 hour, for either turbulence model.

Figure 5 in section 2 demonstrated that the cabin average velocity magnitude decayed within a couple minutes after ventilation shutoff. However, the turbulent kinetic energy in the cabin, which directly affects mass diffusion, did not reach its minimum until much later. Figure 17 shows the effective diffusion vs time for several cases on a logarithmic scale. The black line represents the molecular diffusion coefficient, the theoretical minimum diffusion with no turbulence. The green line represents the effective diffusion in a cabin initialized without airflow (ventilation begins "off") for the $k-\epsilon$ model. The blue and red lines show the diffusion of a typical simulation where the ventilation produces turbulence in the cabin before shutting down at 23 seconds. Using the green line as reference, it takes approximately 30 minutes for the effective diffusion to reach its minimum.

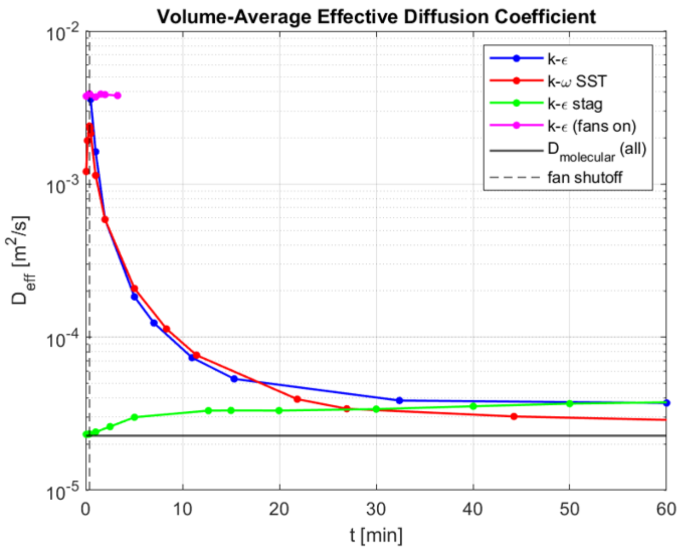

Figure 17. Effective diffusion in cabin over time.

J. Long-Term Results

A handful of simulations were continued beyond 10 minutes. CO_2 produced by the crewmember slowly built up and diffused through the HALO cabin over time, but the highest concentration remained near the crewmember. Figure 18 shows contours of ppCO_2 in mmHg over time for a single crewmember breathing at a wall using the $k-\omega$ SST turbulence model over the course of 2 hours.

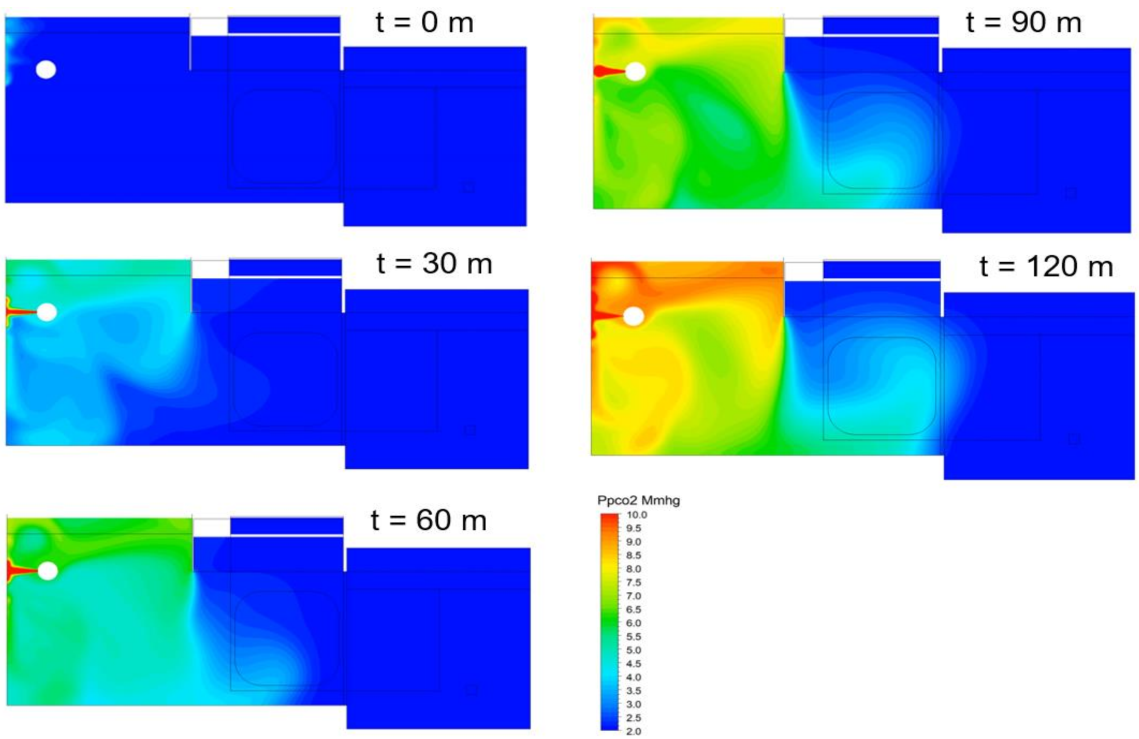

Figure 18. ppCO_2 contours of HARS breathing location using $k-\omega$ SST at various times.

After 1 hour, the CO_2 cloud produced by the crewmember in the HARS position filled the aft section of the cabin, and by 2 hours the cloud had started to fill the middle of the cabin. Figure 19 shows long-term results for flowrate-weighted-average $ppCO_2$ and ppO_2 inspired. One should note that all results were generated from a single crewmember breathing, *except* the light pink and blue dashed lines which represent two crewmembers breathing at the same time in the domain.

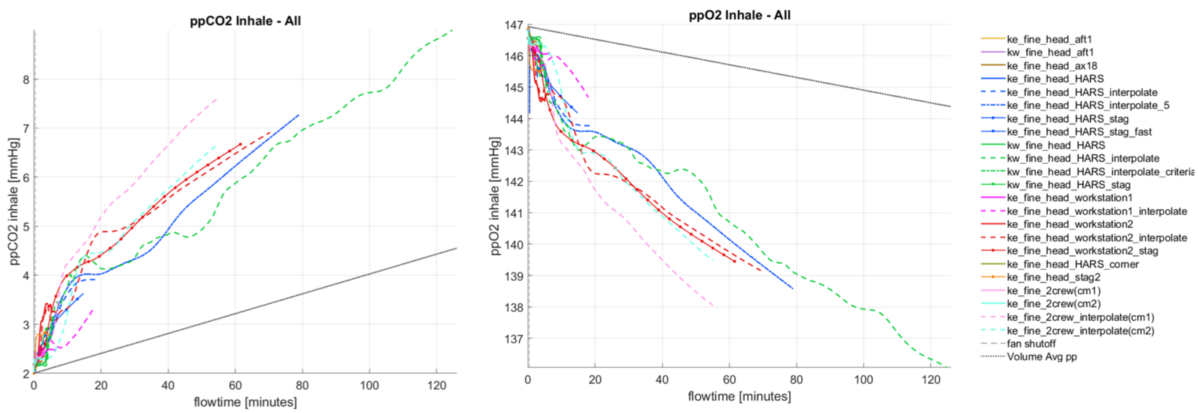

a) Inspired $ppCO_2$ vs time　　　b) Inspired ppO_2 vs time

Figure 19.　$ppCO_2$ inspired (flow-rate-weighted-average partial pressure), long-term results.

After 1 hour the $ppCO_2$ levels for some cases exceed 6.8 mmHg, however they did not exceed the 4-hour maximum allowable time in those conditions according to Table 4. The ppO_2 levels did not reach the 127 mmHg (16932 Pa) limit within this timeframe. Since O_2 is consumed and CO_2 is produced by the crewmember's metabolism, the CO_2 and O_2 trends mirror each other—where CO_2 increases, O_2 decreases. While there is significant variation in inspired $ppCO_2$ and ppO_2 early on, the single crewmember cases start to show more linear behavior later in the simulation.

K. Multiple Crew

To understand how the presence of additional crewmembers breathing would affect inspired CO_2 and O_2, one simulation was run with two crewmembers. The "HARS" location, previously shown in Figure 13 was chosen as the reference case with a single crewmember. A second breathing crewmember was added to the domain, as shown in Figure 20. This crewmember was added in the same plane as the first crewmember but was positioned further towards the middle of the aft segment of the cabin and faced downwards.

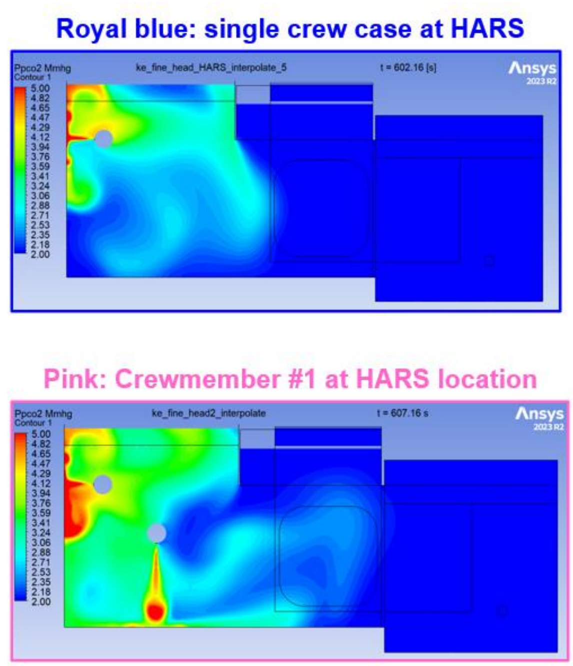

Figure 20.　$ppCO_2$ contours of single HARS crewmember (top) and HARS crewmember with second crewmember (bottom), 10 minutes.

Figure 21 compares the inhaled ppCO2 of the solo crewmember case to a case with two crewmembers, where one crewmember is in the same location as the solo crewmember. At the start of the run, the royal blue line (single crewmember at HARS location) and the pink line (Crewmember #1 at HARS location) tracked the same inhaled $ppCO_2$ until ~7 minutes into the simulation. From this point, the pink line has higher inhaled ppCO2 levels, which is likely due to the second crewmember in vicinity. The time to reach 6.8 mmHg (907 Pa) partial pressure of CO_2 inspired after ventilation turned off was reduced by 28 minutes, shifting from 70 minutes to 42 minutes.

It should be noted that this result cannot be concluded for every case with two crew members breathing, since results depend on proximity and location of the crewmembers.

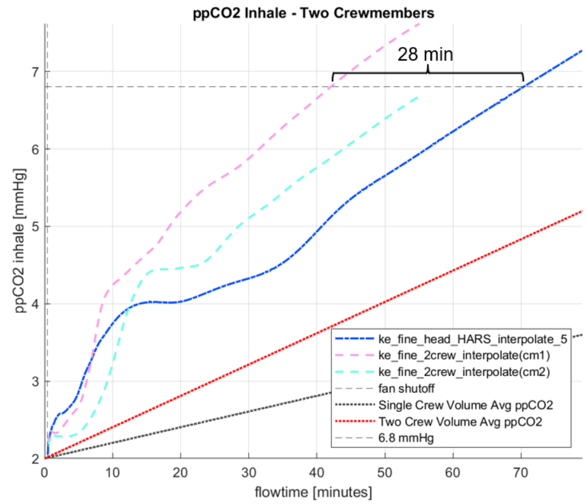

Figure 21. Inspired $ppCO_2$, one vs two crew case.

L. Time-to-Effect Estimations

Time-to-effect is defined as the time until exposure limits and/or durations are exceeded. To estimate time-to-effect for CO_2 and O_2 allowable concentrations, linear regressions were fit to data starting at 30 minutes. As previously noted, the effective diffusion reaches its minimum value around 30 minutes after ventilation turns off. Around this same time, the inhaled concentrations shown in Figure 19 develop a more linear trend than compared to the first ten minutes shown in Figure 14. Figure 22 shows the extrapolations of both CO_2 and O_2 inspired for three different cases. The fine black dashed line represents the volume-averaged concentration, highlighting the fact that the rate of $ppCO_2$ inspired (and ppO_2 depleted) is greater than the volume-averaged rate across the entire HALO module. The worst case was the $k-\epsilon$ turbulence model paired with the HARS breathing location (blue line), reaching 10 mmHg (1333 Pa) $ppCO_2$ in 2 hours. Table 4 specifies the maximum allowable time between 10 and 15 mmHg to be 1 hour. This means that the time-to-effect in which crewmember must vacate the module or don an emergency breathing mask due to CO_2 concentration is 1 hour after 10 mmHg CO_2 is reached, which occurs 2 hours into the simulation. Therefore, the time-to-effect for CO_2 is 3 hours after ventilation off (2 hours to reach 10 mmHg + 1 hour exposure = 3 hours). While lower concentration limits were reached earlier, the exposure time limit was not exceeded. Using the same method of linear regression extrapolation, the ppO_2 limit of 127 mmHg (16932 Pa) would be reached at roughly 3.3 hours. The time-to-effect due to O_2 concentration is 3.3 hours. However, the most limiting time-to-effect is 3 hours due to the CO_2. In

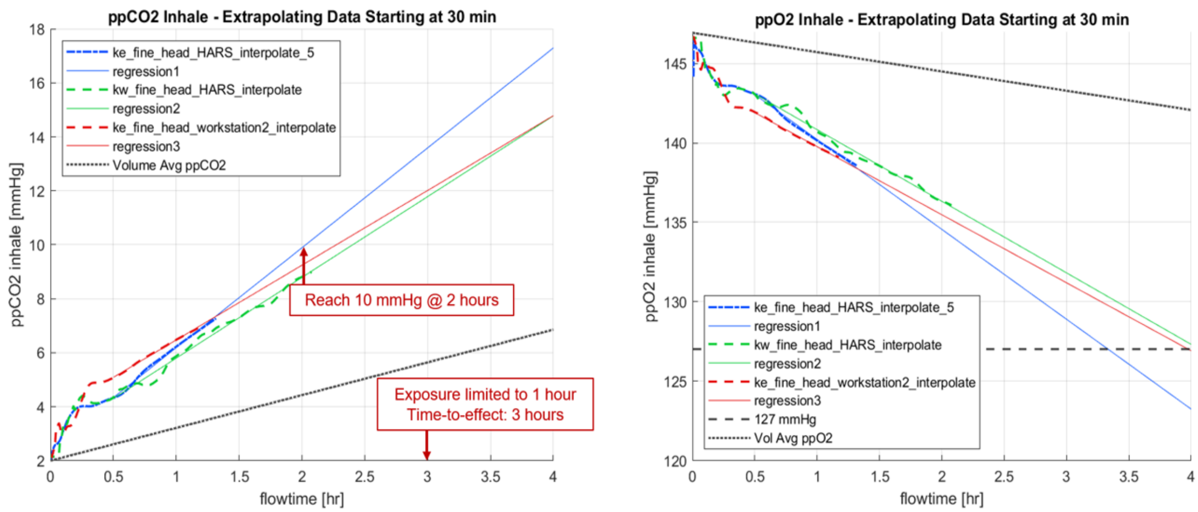

a) Extrapolated $ppCO_2$ inspired vs time

b) Extrapolated ppO_2 inspired vs time

Figure 22. Inhaled partial pressure vs time of CO_2 (a) and O_2 (b).

fact, CO_2 was found to be the limiting factor in all cases. The average $ppCO_2$ of the cabin is shown in Figure 22 and Figure 23, plotted in short black dashes, and represents a perfectly mixed domain, free of concentration gradients. This "solution" is far below the local inspired levels, demonstrating the need for this transient CFD analysis.

Figure 23 shows the estimated time-to-effect for CO_2 inspired by various single crew cases and one two-crew case. The single crewmember breathing against the HARS wall and $k - \epsilon$ turbulence model is plotted in royal blue. For a two-crew breathing case with one of the crewmembers breathing in the exact same spot, the CO_2 inhaled is plotted in pink. Please refer to Figure 20 for further detail. The additional crewmember shifted the worst-case time to reach $ppCO_2$ limits from 2 hr to 1.4 hr, which reduced the time-to-effect of inspired $ppCO_2$ from 3 hr to 2.4 hr.

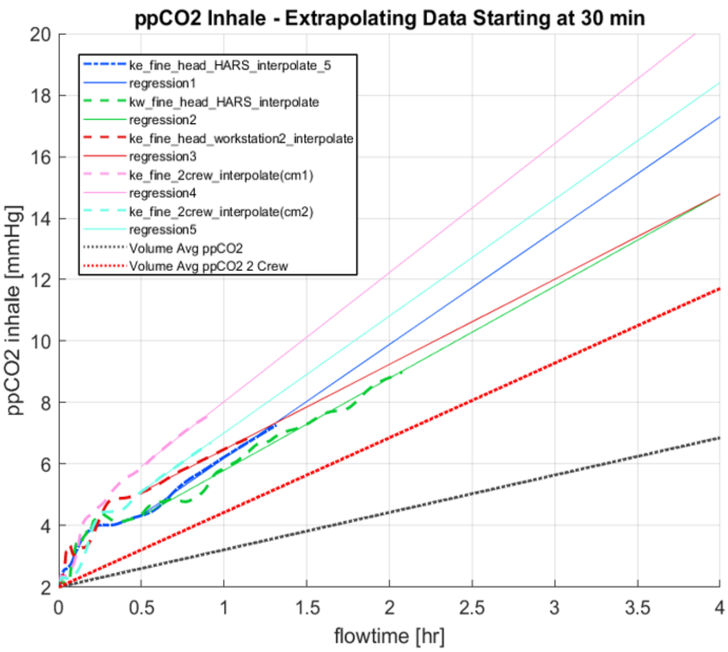

a) extrapolated $ppCO_2$ inspired

Estimated $ppCO_2$ [mmHg]		
t	Single Crew	Two Crew
5 min	2 - 3.5	2.3 - 2.7
15 min	3.6 - 4.6	4.4 - 4.6
30 min	4.3 - 5.8	5.1 - 5.9
1 hr	5.8 - 6.6	7.0 - 8.1
2 hr	8.8 - 9.9	10.9 - 12.4
3 hr	11.8 - 13.6	14.7 - 16.8
4 hr	14.8 - 17.3	18.6 - 21.2

Estimated Time to Reach $ppCO_2$		
$ppCO_2$	Single Crew	Two Crew
10 mmHg	2.0 - 2.4 hr	1.4 - 1.8 hr
15 mmHg	3.4 - 4.1 hr	2.6 - 3.1 hr

b) estimated time-to-effect

Figure 23. Extrapolation of inhaled CO_2 concentrations (a) and estimated time-to-effect (b).

V. Conclusion

While there are many valid reasons for turning off ventilation in an emergency or off-nominal scenario, it is important to make sure the crew is not being put at risk. A CFD model of the HALO module was developed to analyze local concentrations of O_2 and CO_2 inhaled by breathing crewmembers after ventilation is turned off. Various efforts were taken to improve model accuracy and generate a realistic breathing pattern while maintaining computational efficiency. In each case, the time-to-effect for CO_2 was reached before O_2, although not significantly sooner. It was discovered that effective diffusion decayed to its minimum value roughly 30 minutes after ventilation shutoff, which allowed time-to-effect to be estimated by extrapolating data for t > 30 min. Both breathing location and turbulence model were found to affect the results, especially short-term inhaled concentrations (t < 7 min). The worst-case time-to-effect was determined to be 3 hours for a single crewmember. The addition of a second crewmember breathing was found to reduce the time-to-effect to 2.4 hours at the same location. Results from this assessment are being used to inform flight rules and provide insight into how long a crewmember may work in a module without ventilation before they need to seek fresh air or resume ventilation.

There are several options for improving upon this assessment in future work. The human breathing model could be improved from a spherical head and circular mouth to a more realistic mannequin with breathing through their mouth or nostrils. A more accurate breathing model could include the variation of constituent concentrations through the exhale, instead of assuming them constant (please refer to Metabolic Profile and Breathing Pattern section for more detail). This change would increase the CO_2 concentration towards the end of the exhale, which could alter time-to-effect. The accuracy of the RANS turbulence models in capturing turbulence's effect on molecular diffusion is questionable. The results of a large eddy simulation turbulence model on a simplified geometry could be compared to

$k - \epsilon$ and $k - \omega$ SST results on the same geometry to assess any differences in effective diffusion. A wider range of case parameters could be investigated, such as crewmember movement, higher metabolic rates, more locations, and breathing patterns. A portable fan could be modeled with a simple velocity boundary condition to determine if air circulation alone would cause the ppCO_2 inspired over time to be closer to the volume-averaged (plotted in small dashed black and red lines in Figure 23). While this CFD analysis only evaluated scenarios where all ventilation is turned off, scenarios where partial ventilation shutoff occurs could be assessed. The planned future work includes running more cases with up to 4 crewmembers, improving the realism of the crewmember head/body, and evaluating mouth vs nasal breathing.

Acknowledgments

Special thanks to Moses Navarro for the development of the realistic breathing model user-defined function used in this study and guidance during the analysis.

References

[1]Son, C., Ivanov, N., and Smirnov, E., "Numerical Study of Carbon Dioxide Transport Problem for the Open and Lower Airflow Space in the ISS Module," *52nd International Conference on Environmental Systems*, Calgary, Alberta, 2023.

[2]Baukus, A., "Parametric CO2 Washout Sensitivity Assessment for the Addition of the Helmet Absorption Band (HAB)," Jacobs JETS-JE33-22-TLSS-DOC-0032, 2022.

[3]Navarro, M., Conger, B., and Campbell, C., "Exploration EVA Purge Flow Assessment," *41st International Conference on Environmental Systems*, ICES-2023-246, Portland, OR, 2011.

[4]Intagliata, S., Rizzo, A., Gossman, W., "Physiology, Lung Dead Space," *StatPearls*. Treasure Island, FL: StatPearls Publishing, 2023.

[5]Dekker, E., "Transition Between Laminar and Turbulent Flow in Human Trachea," *Journal of Applied Physiology*, Vol. 16, No. 6, 1961, pp. 1060–1064.

[6]"Inlet Values for the Turbulence Length Scale and Turbulent Intensity," COMSOL Multiphysics Reference Manual, version 6.3

[7]"Gateway Subsystem Specification for the Environmental Control and Life Support Subsystem (ECLSS)," National Aeronautics and Space Administration, GP-10004, 2023.